

MITOSIS IN *BARBULANYMPHA*

I. Spindle Structure, Formation, and Kinetochore Engagement

HOPE RITTER, JR., SHINYA INOUÉ, and DONNA KUBAI

From the Department of Zoology, University of Georgia, Athens, Georgia 30602, Program in Biophysical Cytology, Department of Biology, University of Pennsylvania G7, Philadelphia, Pennsylvania 19104, and the Department of Zoology, Duke University, Durham, North Carolina 27708

ABSTRACT

Successful culture of the obligatorily anaerobic symbionts residing in the hindgut of the wood-eating cockroach *Cryptocercus punctulatus* now permits continuous observation of mitosis in individual *Barbulanympha* cells. In Part I of this two-part paper, we report methods for culture of the protozoa, preparation of microscope slide cultures in which *Barbulanympha* survived and divided for up to 3 days, and an optical arrangement which permits observation and through-focus photographic recording of dividing cells, sequentially in differential interference contrast and rectified polarized light microscopy. We describe the following prophase events and structures: development of the astral rays and large extranuclear central spindle from the tips of the elongate-centrioles; the fine structure of spindle fibers and astral rays which were deduced *in vivo* from polarized light microscopy and seen as a particular array of microtubules in thin-section electron micrographs; formation of chromosomal spindle fibers by dynamic engagement of astral rays to the kinetochores embedded in the persistent nuclear envelope; and repetitive shortening of chromosomal spindle fibers which appear to hoist the nucleus to the spindle surface, cyclically jostle the kinetochores within the nuclear envelope, and churn the prophase chromosomes. The observations described here and in Part II have implications both for the evolution of mitosis and for understanding the mitotic process generally.

KEY WORDS mitosis · protozoa · birefringence · anaerobe · culture · microtubule

In studying vital activities of cells, one occasionally encounters bizarre forms which nevertheless uniquely illuminate or illustrate general principles of life. Through his pioneering, now classical studies, L. R. Cleveland pointed out that the life cycles of hypermastigote protozoa, residing in the hindgut of the wood-feeding cockroach *Cryptocer-*

cus punctulatus, exemplify just such a unique gift of nature. The coiling and segregation of chromosomes and the structure of the achromatic mitotic apparatus are exquisitely displayed in these extraordinary anaerobes (e.g. Cleveland, 4, 7).

The hindgut protozoa of *Cryptocercus*, symbionts of the mutualist type, exhibit an extraordinary diversity. Individuals of 30 species fill an anaerobic niche along with equally diverse prokaryotes and particles of ingested cellulose. The protozoa and prokaryotes digest the cellulose in-

gested by the host, making the metabolic products available to it. These microorganisms are unique with respect to their structure, physiology, and reproduction to the extent that one is tempted to regard them as archaic forms resident in a host that itself is a primitive insect (34). *Barbulanympha* is one of 14 protozoan genera in *Cryptocercus*. Four species of *Barbulanympha* dominate the hindgut mass of cells in terms of size, though not in numbers.

Cleveland's remarkable accounts of *Barbulanympha* reveal the potentialities of these species for gaining further insight into the dynamics of mitosis (4-17; see also Hollande and Valentin, 21-25). Specifically, *Barbulanympha* provides (a) a relatively large nucleus with a nuclear envelope that remains intact throughout mitosis; (b) an extranuclear achromatic figure consisting of large, well-separated parts that afford a clear basis for functional interpretation; and (c) synchronous mitosis among individuals, the onset of which is predictable in cells obtained from a host that is close to the time of its molt (4, 13, 16).

Despite Cleveland's extensive and precise descriptions, his studies were limited to light microscope observations of fixed and stained samples, or 15-30-min observations of supra vital cells dying from the presence of toxic oxygen in the atmosphere.

After 15 years of search, Ritter succeeded in developing a synthetic medium permitting long-term culture of the symbiont fauna in an oxygen-scrubbed atmosphere (36, 37). We have since developed a method for microscope slide preparation which permits observation and recording of mitotic events of cultured individuals living for over 3 days.

We now report on several dynamic features of mitosis and fine-structural organization of the achromatic apparatus of *Barbulanympha*. Studies on individual living cells were made by through-focusing with two alternative modes of light microscopy that take advantage of the high contrast, resolution, and image quality now available with rectified polarized light (30, 31) and Smith T system differential interference contrast optics (E. Leitz, Inc., Rockleigh, N.J.). Fine structure was analyzed by polarization optical studies of the birefringent spindles in living cells combined with thin-section electron microscopy of cultured cells preserved with diluted Karnovsky's solution (33).

We confirm Cleveland's descriptions of chromosomal engagement with astral rays by way of

kinetochores embedded in the intact nuclear envelope, and of mitosis in *Barbulanympha* characterized by the absence of a metaphase configuration. We find, in addition, that repetitive shortening of the (chromosomal) astral rays appears to participate in nuclear morphogenesis as well as in chromosome movement to the spindle poles. We also find that mitosis in *Barbulanympha* progresses through two discrete, successive stages, (a) chromosomal spindle fiber shortening to the point at which the nucleus becomes wrapped around the central spindle and the chromosome sets have reached their respective poles without change in central spindle length, and (b) central spindle elongation which induces further chromosome separation accompanied by an intricate topological maneuver of the nuclear envelope, resulting in karyokinesis.

These anaphase events and the dramatic events of nuclear morphogenesis by which *Barbulanympha* completes karyokinesis are described in Part II. A brief synopsis of some of our observations has been published elsewhere (32).

MATERIALS AND METHODS

Culture of the Protozoa

Nymphs of *Cryptocercus* collected in May from the mountains of Georgia and North Carolina were maintained in the laboratory at 13°C. Small blocks of wood, chopped from the water-saturated logs that supplied the collection, provide the environment required for a stock culture. Necessary maintenance is limited to a weekly transfer of wood and cockroaches to a clean, dry container with a tightly fitting lid.

During July and August, individual cockroach nymphs close to molting, molting, or a few hours past molt were selected to provide the inoculum for cell cultivation. These *Barbulanympha* have already been induced by hormone of the host to undergo reproduction in synchrony. At this stage, the hindgut is free of highly birefringent cellulose particles, as the host preparing to molt ceases to feed. Mitotic events of all four species of *Barbulanympha* are uniform (4, 13, 16). Our observations focused primarily on the largest of these species, *Barbulanympha ufulula* (~285 × 205 μm²).

Because of the extreme anaerobic requirement that *Cryptocercus* hindgut protozoa exhibit in their natural environment (12, 36), all precautions are observed for anaerobic maintenance of the synthetic environment. The liquid medium prepared by Ritter contains reduced glutathione (Table I). Inoculation, cultivation, and slide preparation procedures are conducted in a gas atmosphere of 95% N₂ and 5% CO₂, free of O₂ within the range 0.8-20 μM. The mechanical system utilized to maintain this atmosphere is described in detail elsewhere

TABLE I
Cellulose-Free Synthetic Medium* for In Vitro Cultivation of *Cryptocercus* Hind-Gut Microorganisms

	(g/liter)
NaH ₂ PO ₄ · H ₂ O	0.290
KHCO ₃	3.330
KCl	2.494
CaCl ₂	0.820
MgSO ₄ · 7H ₂ O	0.752
d-Glucose‡	0.100
d (+) Trehalose‡	1.000
Glycogen‡	1.000
Casein hydrolysate (enzymatic)§	0.300
Yeast extract	0.100
Loeffler blood serum	0.100
Glutathione (reduced)‡	0.219
Water, glass distilled, to prepare 1 liter	

* pH adjusted to 6.8 with KOH, if necessary.

‡ Nutritional Biochemicals, Corp., Cleveland, Ohio.

§ General Biochemicals, Inc., Chagrin Falls, Ohio.

|| Difco Laboratories, Detroit, Mich.

(37). In brief, this assembly consists of three units connected in tandem; (a) a gas supply and O₂-scrubbing facility, (b) a sealed, glove-box culture chamber, and (c) a gas collecting reservoir that functions as a surge tank.

The medium is prepared, deoxygenated, and introduced into the chamber at a room temperature of 20°C. Working within the chamber, 15 ml of medium is delivered to a 25-ml Erlenmeyer flask, the culture vessel. This provides optimum surface to volume ratio for gas equilibrium. In the anaerobic chamber, the hindgut from the donor is then removed with two stainless steel forceps, one applied to the thorax, the other clamped to the caudal abdominal segment. A quick pull ruptures the intersegmental membranes and allows withdrawal of the entire alimentary canal. Once removed, adhering fat body is teased away from the surface of the relatively large hindgut; the anterior portion is pinched off with forceps at its juncture with the hindgut, as is the segmental remnant posterior to the hindgut (see Cleveland, reference 4 for anatomy). In this condition, the hindgut is dropped into the medium. The hindgut sinks to the bottom of the flask and peristalsis ejects the contents (0.4–0.8 ml, depending on the size of the cockroach) in a manner resembling discharge of paste from a tube. The mass of symbionts gradually scatters over the vessel's bottom, where all but the smallest flagellate species remain. Sterile technique is not observed, and culture vessels remain open to the anaerobic atmosphere. The protozoa continue to grow and reproduce actively under these conditions for an indefinite period, generally exceeding many weeks.

Slide Preparation

Slide preparation for light microscope examination of

Barbulanympha is begun when cultivated cells exhibit the first signs of an achromatic figure, usually 7–10 h after molt at 20°C and 13–18 h at 13°C.

Important considerations for slide preparation include (a) procurement of an optimum volume of liquid containing synchronously dividing cells, (b) adjustment of cover glass height above the slide surface just sufficient for cell immobilization and flattening to achieve optical clarity without inducing trauma, and (c) application of sealant around the sample making possible observation outside the anaerobic chamber for extended periods.

Strain-free slides and cover glasses are utilized in these procedures (M6145 slides from Scientific Products Div., American Hospital Supply Corp., McGraw Park, Ill.; Selex 18 × 18 mm cover glasses from Dolbey Scientific Co., Philadelphia, Pa.). The slide and cover glasses as well as glassware for cultivation are cleaned to avoid contaminating materials of all categories, including even minor specks of lint. This cleaning method, which is a prerequisite to studies of living cells with rectified polarization optics, is reported elsewhere (20).

Our slide chambers contain *Barbulanympha* cells appropriately flattened and uniformly distributed. This is managed by collecting a 50-μl vol of medium and cells from the bottom of the culture flask and transferring this volume to a 450-μl plastic microcentrifuge tube. *Barbulanympha* quickly settle by gravity into the conical bottom. A 5-μl volume of bottom solution is drawn into a 3-cm length of 0.58 mm inside diameter polyethylene tubing fitted to the tip of a calibrated Hamilton microsyringe and transferred to an 18-mm square cover glass.

The 18-mm square cover glass is previously prepared to receive the sample. A 1.7-mil (43 μm) polyethylene membrane, with a square hole 14 mm to the side, is cut to conform to the outside dimensions of the cover glass. The frame remaining is 2 mm wide on each of its four sides. This spacer is aligned with the edges of the cover glass and applied to the glass surface previously rimmed with a small amount of silicone grease (high vacuum grease from Dow Corning Corp., Midland, Mich.). Uniform pressure from a flat tool moved around the surface of the spacer squeezes out excess grease and gas bubbles. The exposed face of the spacer is then rimmed with more silicone grease.

With the 5-μl sample delivered to the center of the well formed by this assembly, a glass slide is carefully centered and lowered to contact the sample. For optimum compression (to ~100-μm thickness) of the large *Barbulanympha* cells, the sample should spread to a drop approximately 8 mm in diameter as the slide is gently pressed down to complete the silicone seal. Finally, the slide culture prepared in the anaerobic chamber is removed for subsequent examination in room atmosphere.

In practice, a number of slide cultures are prepared to provide a large number of cells from which to select those in suitable orientation for study. Except for occasional preparations in which cells fail to complete their

cycle, most acceptable slide cultures contain viable cells up to 3 days. This time greatly exceeds the time required for *Barbulanympha* to complete its cell division.

Microscopy

Observations were made on individual dividing cells alternately with polarized light and differential interference contrast microscopy. Rectified 20× and 40× Nikon objective lenses (Nikon Inc. Instrument Div., Garden City, N. Y.) were used for polarized light, and 16× and 40× Leitz Smith T system objectives were mounted on the same quadruple revolving nosepiece¹ for differential interference contrast microscopy. A strain-free condenser for the Leitz differential interference contrast system, with turret mounted Wollaston prisms and blank space, served for both types of microscopy. The optical components of the inverted microscope were mounted on a rigid cast steel vertical optical bench designed by us (29). Collimated light from a 100-watt concentrated mercury arc lamp (#110 from Illumination Industries, Inc., Sunnyvale, Calif.), filtered through two heat cut filters (#4602 from Corning Glass Works, Science Products Div., Corning, N.Y., or #4010 from Edmund Scientific Co., Barrington, N.J.) and a 546-nm narrow band pass interference filter (#10-98-2 from Baird Atomic, Inc., Bedford, Mass.) was linearly polarized by a Glan-Thompson calcite prism (20 mm square from Karl Lambrecht Corp., Chicago, Ill.). A rotary sheet of mica $\lambda/25$ in retardation and placed before the condenser, and a second Glan-Thompson prism with directly cemented stigmatizing lenses mounted in the body tube, served as compensator and analyzer for both polarized light and differential interference contrast.

With the optical system described, one can quickly switch between rectified polarized light and differential interference contrast observations by rotating the quadruple nosepiece and condenser turret. Also, by adjustment of the $\lambda/25$ Brace-Köhler compensator, some spindle birefringence can be detected, superimposed on the differential interference image. For differential interference contrast not used at peak sensitivity, or near extinction, a third swing-out polarizer built into the Leitz condenser was introduced to attenuate image brightness and reduce the intensity of illumination reaching the specimen. For observations or time-lapse photography over several hours, we found that cells proceed through division better and especially enter anaphase-B more readily when illumination is further reduced by 2-3 sheets of an amber filter (#5 from Kliegl Bros., Universal Electric Stage Lighting Co., Inc., Long Island City, N.Y.). These filters may have reduced any stray short

¹ The Leitz Ortholux quadruple nosepiece was modified by Mr. Edward Horn of the University of Pennsylvania, Biology Instrument Shop, according to his unique design, so that each of the four objective lenses can be independently rotated in its place without decentration.

wavelength visible light or long wavelength ultraviolet, or may have simply acted as an attenuator for the 546-nm mercury green light. Eventually, our best records were obtained by mounting one to two such filters on a solenoid shutter synchronized to move out of the light path with each exposure of the still and movie cameras, another amber filter being fixed permanently in the light path.

Serial, through-focus 35 mm still pictures were taken on Kodak Plus-X film with a Nikon Automatic Microflex motor-driven camera with the beam splitter oriented at 45° to the analyzer transmission direction. The film was developed at 18°C in 1:3 dilution Kodak Microdol X. Time-lapse 16 mm films were taken with an Arriflex camera on Kodak Plus-X negative film and processed commercially. All observations were made in a room thermostated to 18° ± 1°C.

For electron microscopy, organisms were prepared as described by Kubai (33), except that the more dilute first fixative contained 0.036% paraformaldehyde, 0.23% glutaraldehyde, and 0.02M phosphate buffer, pH 7.0.

RESULTS

Development of Astral Rays and Central Spindle

Approximately 18 h after inoculation of *Barbulanympha* into culture, two prominent, elongated structures are evident at the anterior end of the organism beneath the flagellar tuft (Fig. 1). These elongate-centrioles exhibit positive birefringence and extend in a postero-lateral direction from their origin near the medial end of the corresponding parabasal-axostylar lamella (Figs. 1, 2a, b, 3a, b). A spherical centrosome ~8.5 μ m in diameter surrounds the posterior tip of each elongate-centriole (Figs. 1, 2a, b, 3a, b). Although not easily detectable at this early stage, astral rays radiate from the centrosomal surface. These can be seen by phase contrast (Fig. 1), differential interference contrast (Fig. 3a), and polarized light (Fig. 3b) microscopy. Furthermore, in polarized light the positive birefringence of the astral microtubules can be traced through the centrosome to their origin at or near the tip of the elongate-centriole (Figs. 3b, c; see also text figure 20 in reference 4). The astral microtubules arise from the tip of the elongate-centriole, extend through the centrosome, and coalesce to form refractile fibers visible with phase and interference contrast optics beyond the centrosomal surface.

As described in fixed and stained preparations and in living cells by Cleveland (4, 5, 14, 17), some of the astral rays from the two elongate-



FIGURE 1 Phase-contrast micrograph of *Barbulanympha* very early in division. The nucleus (*N*) still lies some distance away from the two bulbous centrosomes (*S*). The centrosomes cap the distal tips of the elongate-centrioles (*E*) which are seen as prominent twisted rods at the anterior end of the organism. Asters (*A*) radiate from the centrosomes. The converging proximal ends of the two elongate-centrioles bend medially and merge with the parabasal axostylar lamellae (*L*), seen in this optical section as thin dark lines running at the base of the flagellar kinetosomes. The left and right flagellar tufts (*T*) have not yet started to separate. Many species of protozoa cohabiting the wood cockroach intestine crowd around the *Barbulanympha*. Bar, 10 μm . $\times 1,370$.

centrioles become aligned parallel to each other and coalesce to form the early central spindle fibers. As seen in our Fig. 3*a* and *b*, some of these fibers originate at the tip of the elongate-centrioles and others arise at additional loci some distance proximal (anterior) to the centrosomes. With time, the number and length of astral rays, as well as number of fiber bundles which make up the central spindle, progressively increase as manifested in the striking rise in their birefringence (Figs. 3*c, d, 4a* to *d*).

The developing central spindle often bows anteriorly while further fibers are added between

this part and the nucleus located somewhat posteriorly (Fig. 3*c, d*). This pattern of spindle fiber formation may be responsible for the bipartite organization and helical arrangement of the fibers found in the mature central spindle. During these earlier stages of spindle development, the birefringence of astral and central spindle fibers remains converged to the elongate-centriolar tip.

Progressively, more fibers are added until eventually the central spindle reaches its full length, diameter, and birefringence (Fig. 4*a* to *d*). Once the spindle has thus matured, these parameters remain unchanged until the end of anaphase-A,

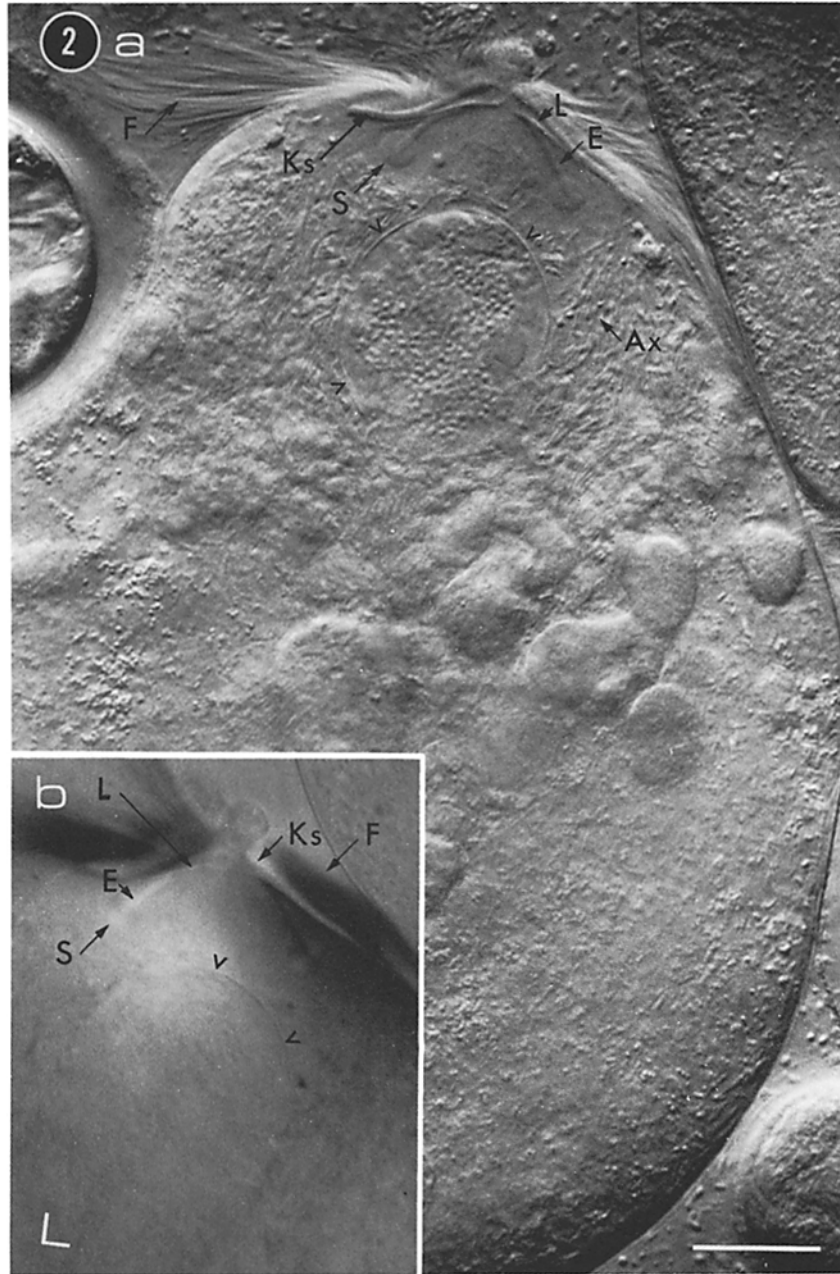


FIGURE 2 (a) Differential interference contrast image of *Barbulanympa* early in prophase. The organism was flattened for observation. Chromosomes are condensing within the nuclear envelope (v's). One spherical centrosome (S) each caps the distal tips of the two elongate-centrioles (E). The base of the elongate-centrioles merge with the parabasal axostylar lamellae beneath the rows of flagellar kinetosomes (Ks). Asters are not obvious. Instead, long thin parabasals and axostyles (Ax) which trail posteriorly from the parabasal axostylar lamellae surround the nucleus. (b) inset, polarized light image of anterior portion of the same individual. Most of the flagella (F) which run in the NW and SE quadrants appear in dark compensation as do the right hand elongate-centriole and parabasal axostylar lamella. In contrast, the right hand row of kinetosomes (each kinetosome is oriented perpendicular to the row), the left hand elongate-centriole, and the adjoining region of the parabasal axostylar lamella appear in bright compensation. Each flagellum, kinetosome, elongate-centriole, and parabasal axostylar lamella, as well as the nuclear envelope (cf. esp. Fig. 3 b, c, d), all display tangential positive birefringence. At the compensator setting used to take this photograph, sectors of the centrosomes in the NW and SE quadrants appear dark, and in the NE and SW quadrants they appear bright. This pattern reflects the positively birefringent material which is oriented radially in the centrosomes. L: Axes of crossed polarizer and analyzer and quadrant containing the compensator slow axis. Bar, 30 μm . $\times 570$.

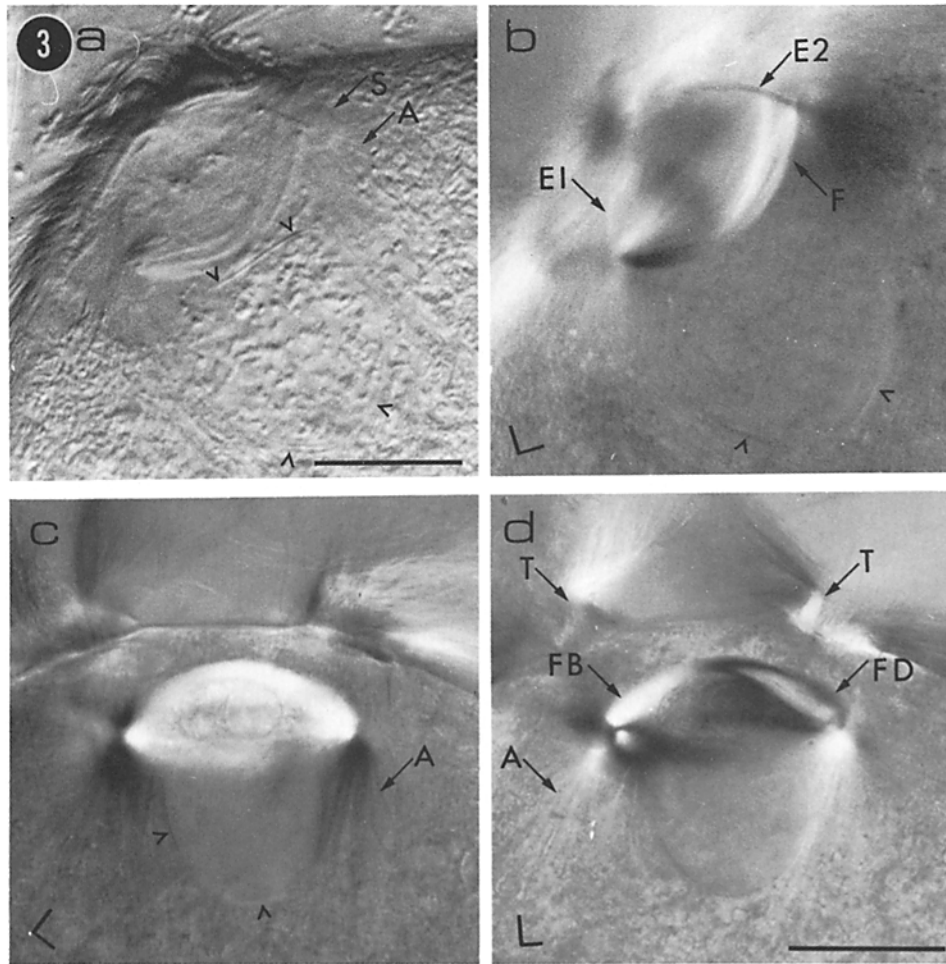


FIGURE 3 Early spindle formation. (a) Differential interference contrast. (b) Polarized light image of the same cell. (c, d) Another cell at a somewhat later stage both in polarized light but with polarizer and compensator axes oriented differently. *L*, axes of crossed polarizer and analyzer and quadrant containing slow axis of compensator. In (a) and (b) bundles of spindle fibers (*F*), which were formed by merging astral rays growing from opposing elongate-centrioles, show as segments of arcs running between the elongate-centrioles. In (b), the right elongate-centriole (*E2*) appears threadlike in dark compensation, the left one in bright compensation (*E1*). The flagellar tufts have not yet separated so that the two elongate-centrioles converge anteriorly. Some spindle fibers originate at the distal tips of the elongate-centrioles, others arise more proximally. In the differential interference contrast image (a), astral rays (*A*) which are not incorporated in the central spindle can be seen as if radiating from the (right hand) centrosomal surface (*S*). However, the polarized light images show that the birefringent microtubules of these newly formed astral rays in fact run through the centrosome and reach the elongate-centriole from whose surface they originate (b). In (a), the optical section of the nuclear envelope (*v*'s) appears shield-shaped. The nucleus has been drawn closer to the extranuclear spindle, and a segment of the envelope appears as a straight line where it is apposed to the spindle. The parabasals and axostyles have not yet fully contracted and appear as mottled birefringent structures to the left and right of the nucleus in (b). In (c, d), the flagellar tufts (*T*) have separated. The spindle, though still not yet fully mature, exhibits a higher birefringence now being made up of many more fibers. Spindle fiber bundles appear bright (*FB*) where they run parallel to the slow axis of the compensator and generally dark (*FD*) where they run in the opposite quadrants. In (d), however, white "eyes" appear in the middle of the dark fiber bundles (lying in the NW and SE quadrants) where the fiber concentration is so high that the spindle retardation far exceeds the effective retardation introduced by the compensator. (See 40, for how the compensator setting affects the appearance of the image of mitotic spindles). The spindle appears bipartite possibly because fiber formation is obstructed in the middle by the nuclear sleeve (structure seen in the middle of the spindle in (c) and (d)?). The astral rays (*A*), especially those running posteriorly and parallel to the nuclear envelope, have grown in number, length, and birefringence. They appear in dark compensation in (c), and are bright in (d). Bar, 30 μm . $\times 690$.

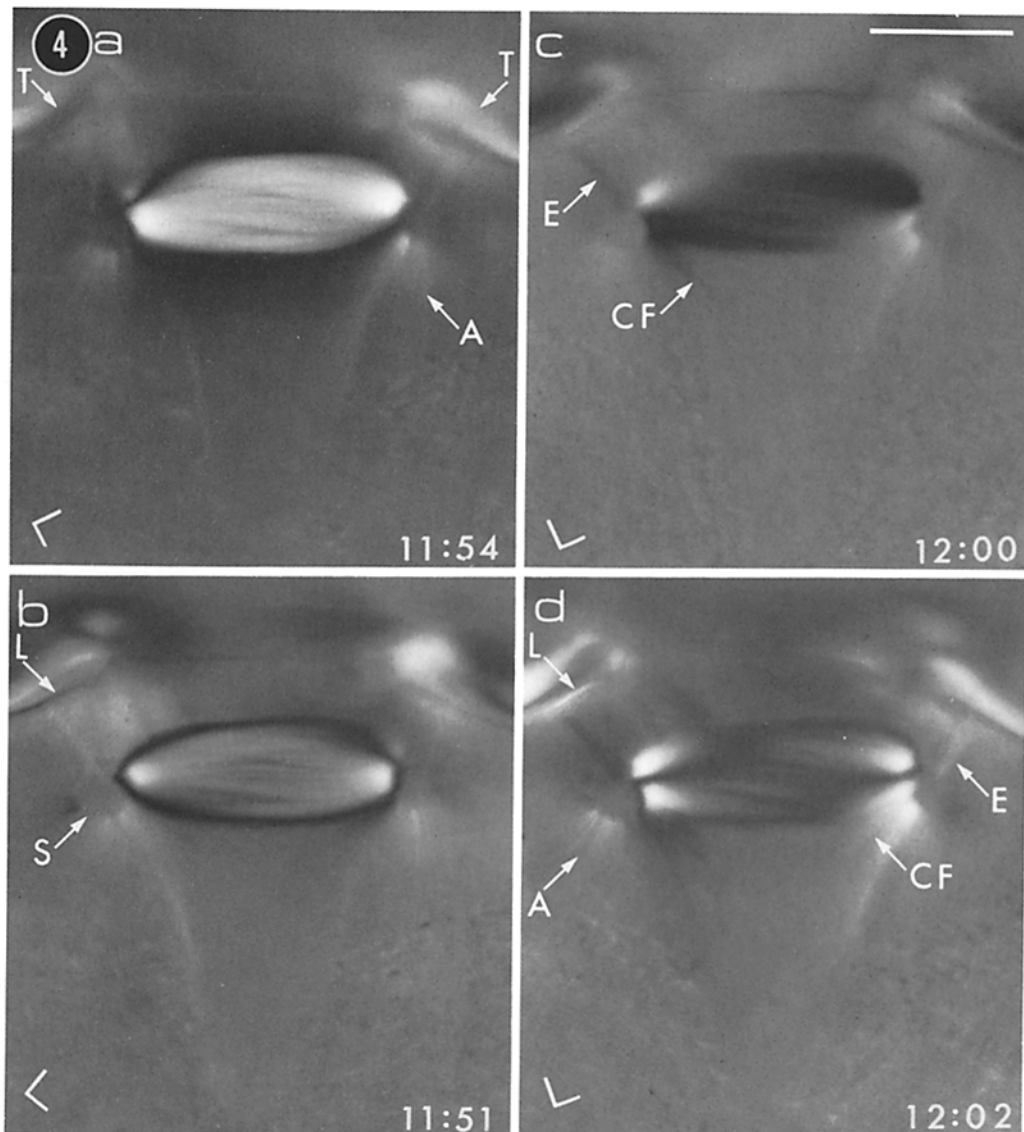


FIGURE 4 Birefringence of mature, central spindle in prophase. Flagellar tufts (*T*) and their basal structures are now sufficiently separated so that the elongate-centrioles (*E*) diverge anteriorly. All four pictures were taken with Nikon 40x rectified polarized light objectives, with crossed polars and compensator axes oriented variously relative to the spindle axis. *L*, Axes of crossed polarizer and analyzer and quadrant in which compensator slow axis is oriented. These photographs show how the central spindle is clearly composed of birefringent fiber bundles which are somewhat twisted relative to the spindle axis. Compare with electron micrograph Fig. 5. Where the concentration of fibers is greatest, adjacent to the centrosomal surface, individual fibers are not resolved and the birefringence is highest. Both spindle and aster birefringence appear to terminate at the surface (*S*) of the spherical centrosome, but in fact a weak, radially positive birefringence exists within the centrosomes (cf. Fig. 2*b*). The dark conical tip seen at the left spindle pole in (*b*) is in fact made up of birefringent fibers which continue from the central spindle through the centrosome and terminate at the tip of the elongate-centriole. (Also, see in Part II, Figs. 2*a*, *b*, *f* and 14*a*, *c*, *e*, and *f*). In (*b*), the fibers of the central spindle outside of the centrosome are more birefringent; they possess the same sign of birefringence, and also lie in the same orientation as the fibers within the centrosome, but they overcompensate and appear bright. In (*b*), the distal portion of the left hand elongate-centriole appears in bright compensation. In (*a*), (*c*), and (*d*), it appears in dark compensation. The distal portion of the right hand elongate-centriole which is mostly out of focus appears in bright compensation in (*a*), (*c*), and (*d*). Long astral rays (*A*), some running tangential to the teardrop-shaped nucleus, are seen in bright compensation in (*a*), (*b*), and (*d*). In (*c*) and (*d*), what appear to be short astral rays which converge postero-medially towards the spindle axis are in fact chromosomal spindle fibers (*CF*). They terminate abruptly on kinetochores which are permanently embedded in the nuclear envelope. Although difficult to photograph, a miniature, radially positive spherulite is visible in the rectified polarizing microscope at the tip of each of these astral rays. These spherulites are in fact the kinetochores. Time in h:min of day on 74g26. Bar, 30 μm . $\times 630$.

when all of the chromosomes have arrived at the spindle poles (see Part II).

Structure of the Mature Spindle

A fully mature central spindle takes on the configuration illustrated in Figs. 4*a* to *d* and 7*a* to *c*. These polarized light images show varied specimen and compensator orientations (relative to the crossed polarizers) to emphasize different structural features. Birefringent fibers that correspond to bundles of microtubules in the central spindle are especially clear in Fig. 4*b*. They diverge near the spindle axis and give rise to a helical appearance in polarized light. The more intense pericentrosomal birefringence reflects the higher packing density of these microtubules toward the spindle poles.

The grouping of microtubules into thin bundles, their helical course, and their higher packing density at the centrosomal surface are also apparent in electron micrographs (Figs. 5 and 6).

The long astral rays, some of which run posteromedially tangential to the nuclear envelope, can be seen in varying contrast in Figs. 4*a* to *d* and 7*a* to *c*. Some of the astral rays which terminate on the chromosomal kinetochores, embedded in the persistent nuclear envelope, are seen as medially pointing, discrete strands in Figs. 4*c*, *d* and 7*a* to *c*.

The centrosomes are now sharply outlined by the astral rays and spindle fibers (Figs. 4*a* to *d* and 7*a* to *c*) in contrast to their earlier appearances seen in Fig. 3*b* to *d*. The birefringence of the microtubular bundles now appears to end abruptly at the centrosomal surfaces. Although much of the birefringence no longer penetrates the centrosome, closer inspection with appropriate compensator adjustment reveals that in fact some positively birefringent strands do reach the tip of the elongate-centriole. Some of the central spindle fibers and astral and chromosomal microtubules are still connected to the centriolar tip embedded in the centrosome (Figs. 4*b*; and in Part II, 2*a*, *b*, *f*, 14*a*, *c*, *e*, *f*, 15*f*, *h*). Some microtubules can be seen likewise within the centrosome in the electron micrograph (Fig. 5).

With time, the two tufts of flagella and the parabasal-axostylar lamellae move apart and the anterior bases of the elongate-centrioles diverge (Figs. 3*c*, *d*, 4*a* to *d*, 7, 8*a* to *c*). In Figs. 4*c*, *d*, and 7*a*, the two elongate-centrioles are oriented at 90° to each other in opposite quadrants, hence

appearing in dark (left) and bright (right) contrast in the compensated polarized light image.

Chromosome and Nuclear Hoisting

During or shortly after central spindle maturation, some astral rays are seen terminating on the chromosome kinetochores which are embedded in the persistent nuclear envelope. These rays, now designated chromosomal spindle fibers (Figs. 4*c*, *d*, 7*a* to *c*, 8*a*, *b*), appear to form and contract repeatedly. In the posterior tapered region of the nucleus that otherwise appears empty, chromosomes are occasionally observed with their kinetochores displayed in the lateral margins of the nucleus (Fig. 1*a* to *d* in Part II). Such a kinetochore with its chromosome travels along the nuclear envelope towards the adjacent spindle pole for several tens of micrometers until they merge with the majority of chromosomes. In a few minutes, another chromosome, not earlier evident, again appears in the "empty" region, displaying its kinetochore in the lateral nuclear envelope, and repeats that poleward migration. Reflecting these movements, time-lapse motion pictures show the chromosomes in *Barbulanympha* prophase to churn violently within the nucleus.

On the whole, the chromosomes move kinetochore foremost, first toward the side of the spindle and then repetitively toward the spindle poles. Chromosomes at this prophase stage are shown in differential interference contrast in Fig. 7*d* to *f*.

As the kinetochores are drawn toward the spindle and to the spindle poles, so also is the nuclear envelope hoisted forward. In Fig. 7*d* to *f*, the anterior margin of the nuclear envelope has wrapped about halfway around the spindle. By the stage shown in Fig. 8, the nucleus has completely wrapped around the central spindle. The posterior margin of the nucleus at this stage often takes on an inverted bell shape, or the shape of a hanging bubble.

In detail, the nuclear envelope is dynamically deformed at each kinetochore insertion. In Part II, we document these deformations and analyze the force operating on the kinetochores and the nuclear envelope after we describe the events of the two-stage anaphase, nuclear morphogenesis, spindle, and aster dynamics and cytokinesis.

DISCUSSION

Successful cultivation of the anaerobic, hindgut protozoa of *Cryptocercus* now enables us to follow

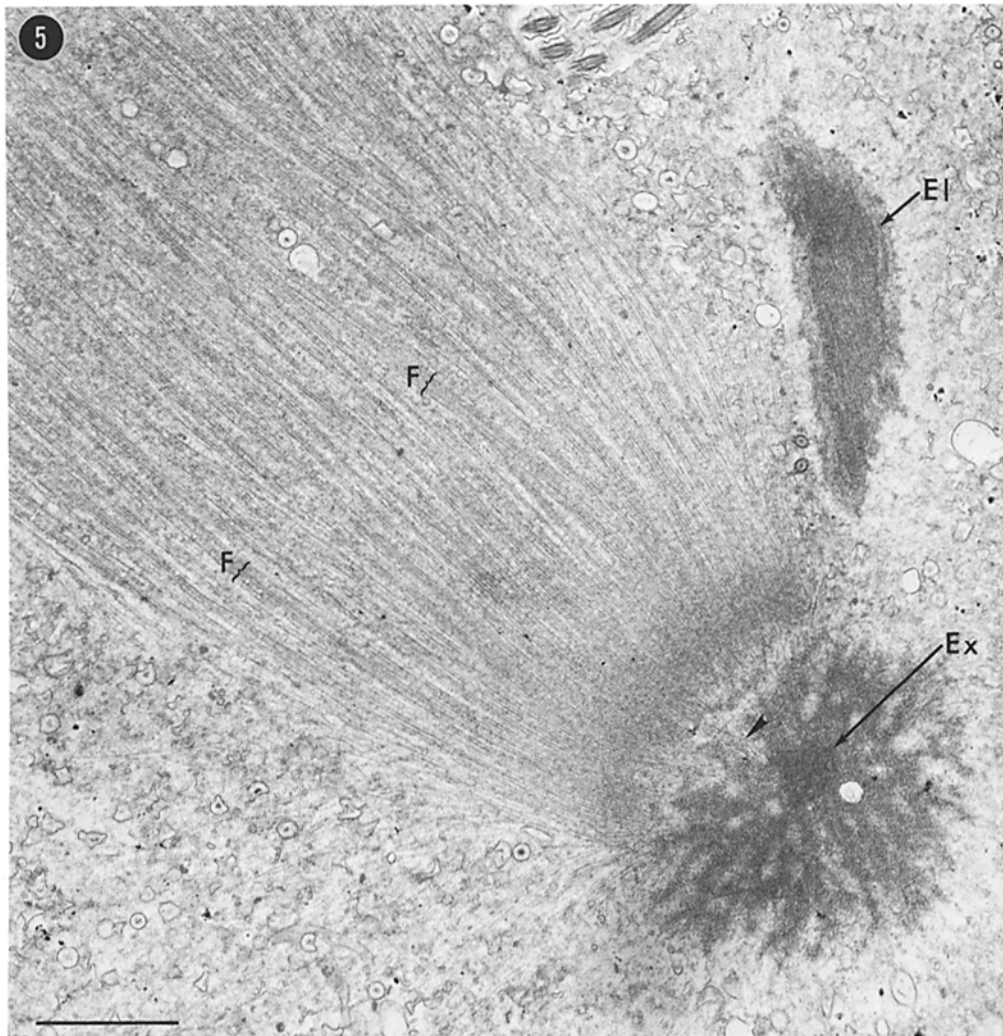


FIGURE 5 Low-power electron micrograph of relatively young central spindle, centrosome, and portions of elongate-centriole. The fibrous elongate-centriole seen in longitudinal section in the upper right (*E*) bends (medially) towards, rather than away from, the spindle equator. Thus, the flagellar tufts have apparently not yet separated. The amorphous centrosome (lower right) shows an irregular radiating pattern and no limiting membrane. The dense core seen in the centrosome is a cross section of the elongate-centriole (*Ex*) near its tip. The elongate-centriole may contain microtubules, but the cartwheel-like arrangement characteristic of centrioles in other organisms has not been observed. The disposition of microtubules in the central spindle correspond exactly to that deduced from polarized light observations in vivo. The microtubules are clustered into longitudinal bundles, namely the continuous spindle fibers (*F*). They in turn form upper and lower spindle portions which are somewhat twisted relative to each other and to the spindle axis. Near the centrosomal surface, the microtubules of the central spindle are highly concentrated and microtubules no longer appear clustered into bundles (i.e., into discrete spindle fibers). This accounts for the higher birefringence, and also the radial disposition of the birefringence axis in the pericentrosomal central spindle. From this region, a few bundles of microtubules can be seen penetrating the centrosome and reaching the elongate-centriole (arrowhead). These microtubules apparently account for the weak radially positive birefringence in the centrosomes. Astral microtubules are visible above the central spindle, below the longitudinal section of the elongate-centriole. Other microtubules appearing below the spindle are presumably reaching out towards the nucleus. Bar, 2 μm . $\times 9,450$.



FIGURE 6 Higher magnification electron micrograph of a portion of the central spindle shown in Fig. 5. To the right, the microtubules converge towards the centrosomal surface. From the middle left to the lower right margins of the picture, one sees the junction of the intertwined bundles of microtubules. Lateral arms of microtubules are not obvious in this picture but are present. They appear prominently when two transparencies of this same photograph are superimposed and displaced along the microtubule axis by 1.5 to 3 times the microtubule diameter (See Fig. 16 in Inoué and Ritter, 32). Fixed in diluted Karnovsky's solution (33). Bar, 500 nm. $\times 29,200$.

dynamic events of division in individual *Barbulanympha* cells.

The anaerobic cultivation system, the nutrient medium, and techniques utilized in maintaining *Barbulanympha* in vitro are the result of many years of effort. Details of the chemical medium that supports growth and reproduction of *Cryptocercus* hindgut protozoa will be described in a separate publication along with cultivation techniques. Table I lists the composition of the cellulose-free medium specifically applied to these studies. The culture chamber and associated equipment, assembled for regulation and maintenance of an O₂-free gas atmosphere, is now an adequate substitute for the physical environment provided by the hindgut. This system facilitates limited microscope observations and experimental procedures requiring an atmosphere containing as little as 0.8–20 μM O₂ (37).

In contemplating the application of highly refined optics to *Barbulanympha* studies in vitro, it became obvious that this cultivation chamber would not be readily adaptable. As a first alternative, a perfusion chamber was mounted on the stage of the inverted optical-bench microscope designed by Inoué and Ellis. Although perfusion chambers designed by Dvorak (19) and Ellis² were tried, neither was satisfactory for this application. However, in these trials, several requirements for prolonged microscope observation of *Barbulanympha* cells became evident. (a) A seal or chamber wall made of silicone grease was harmless and sustained activities of crowded *Cryptocercus* protozoa and prokaryotes for several days. In spite of the high oxygen solubility of silicone grease, and perhaps because of an even higher solubility of carbon dioxide, the collection of microorganisms appeared able to maintain the strict anaerobic environment within the microchamber. (b) Compression of the large *Barbulanympha* cells to ~100-μm thickness provided optimal combination of optical clarity and suppression of movement while affording good viability. As shown in Fig. 8d, *Barbulanympha* are covered with bacterial symbionts (see also 25, 38). The microscope image becomes fuzzy unless growth of a thick lawn of bacteria on the slide and cover glass surfaces is prevented by compression of the *Barbulanympha* held against these surfaces.

These findings suggested that the conditions required for prolonged observation of individual dividing cells could be met most simply with a

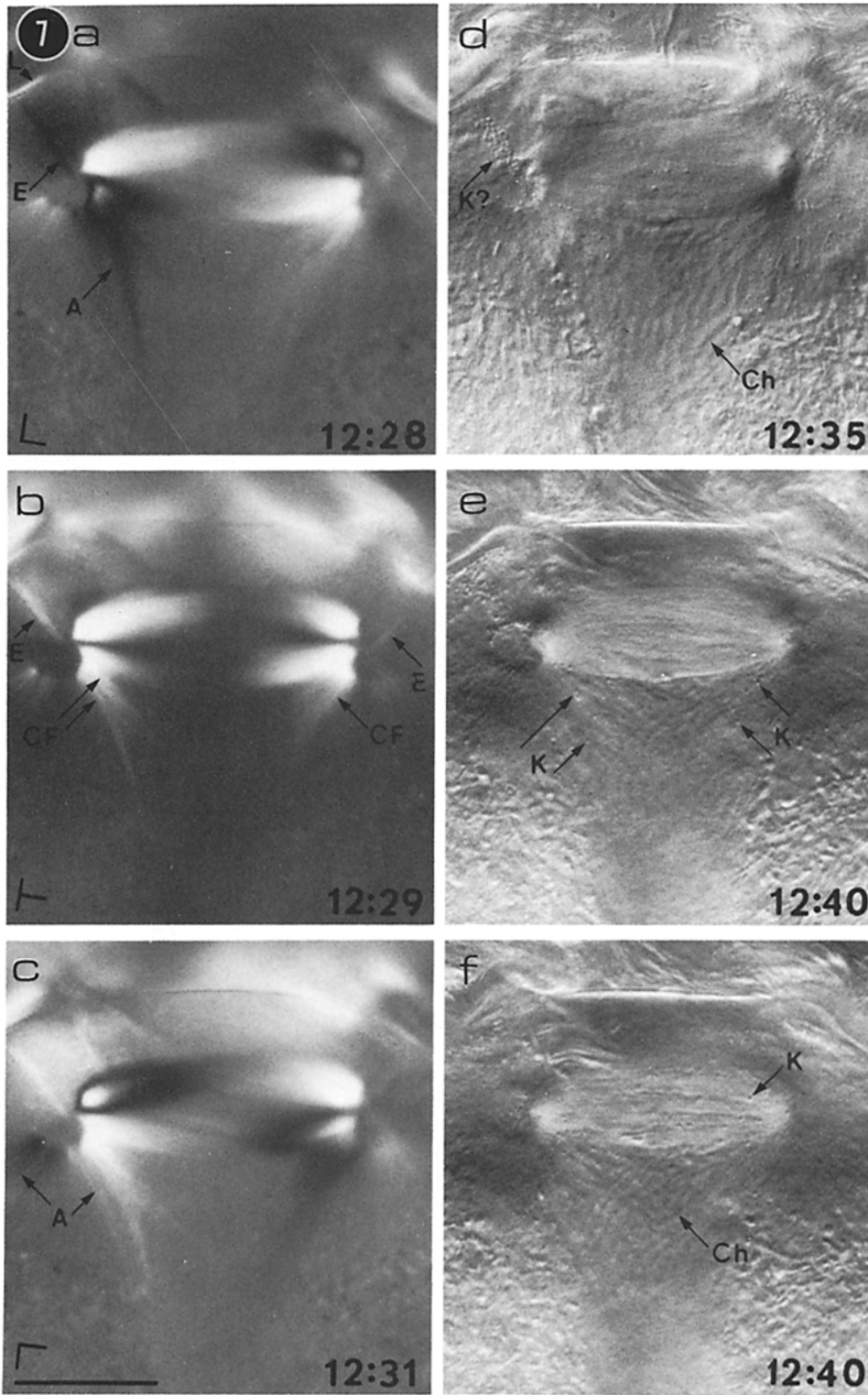
² An unpublished, compact design perfusion chamber.

silicone grease-sealed slide chamber in the absence of perfusion. This led to the design of the slide culture chamber employing a 1.7-mil thick polyethylene spacer-gasket as described.

For observations with the light microscope, we chose to combine rectified polarized optics with the Leitz Smith T system. With polarized light optics, the birefringent achromatic regions of the mitotic apparatus are vividly displayed. Furthermore, the axes and magnitude of birefringence permit interpretation of the fine structure, changes in which can be followed with time (review, 29, 32). The T system differential interference contrast optics provides a crisp, shallow depth-of-field image displaying refractive index boundaries in relief with little interference from out-of-focus objects.

As results indicate, the combination of these two systems mounted on a common microscope base enabled recording both "achromatic" and "chromatic" structures in considerable detail. Through-focus observations (e.g. Fig. 12 in Part II) with these optical methods provide both visibility of image detail and the opportunity for uninterrupted observation lasting many hours. Hughes and Swann (27) first used phase-contrast and polarized light alternately to study mitosis in chick fibroblast cells. Improvements in microscope optical systems through the intervening years, as well as the larger size and unique features of mitosis in the *Barbulanympha* cell, have provided us with much more detailed information than that contributed by earlier workers.

We have noted with particular interest the similarity of the electron microscope appearance of the central spindle compared to its polarized light image and the fine structure deduced therefrom. This consistency should be expected in view of the contribution of microtubules to the formation of spindle fibers and astral rays (review, 29, 32), and to the accounting of their form birefringence (39, 40). Nevertheless, in view of the skepticism expressed by some regarding the interpretation of spindle birefringence, it is gratifying to find that the exact disposition of microtubular bundles deduced from our rectified polarized light images in vivo is, in fact, precisely depicted in Kubai's thin-section electron micrographs of the *Barbulanympha* spindle (Figs. 5 and 6). The very high pericentrosomal birefringence of central spindle fibers and astral rays, and the low birefringence within the centrosome of the mature anaphase-A spindle are likewise revealed in the microtubule distribution seen in the electron micro-



graphs.

For the earlier stages of spindle formation, we described the convergence of birefringent fibers to a point at the posterior tip of the elongate-centriole. We believe this to be a reflection of the microtubule organizing capability of the elongate-centriole. Later in division, centrosomal birefringence decreases (e.g., compare Fig. 3*b, d* with Figs. 4 and 7*a* to *c*). This seems to reflect the reduction of microtubules which reach the elongate-centriole as the spindle fiber and astral ray organizing centers presumably migrate to the surfaces of the centrosomes. This may well represent a rather general phenomenon. In the early stages of division in many marine eggs and insect spermatocytes, spindle fibers and astral rays converge to a point so small as not to be resolvable in the polarizing microscope. (It should be noted that, even limited by the wavelength of light, rectified polarization optics affords a resolution of ~200 nm). Shortly after spindle formation, the birefringent fibers can be seen to terminate farther away from the spindle poles (28).

In careful studies of electron micrographs, many have questioned whether mitotic microtubules, in fact, reach or grow from the centriolar surfaces. Much has been made of the fact that microtubules are commonly found to grow from pericentriolar satellites rather than directly from the surface of the centrioles (43). However, Brinkley and Stubbs (3) have found that, in the early stages after recovery from colchicine or cold depolymerization of microtubules, the newly formed microtubules, in fact, do grow attached directly to the centriole as far as electron microscope resolution permits one to decide. These electron microscope findings are consistent with our interpretation that microtubules initially grow directly from centrioles and that later the organizing centers migrate some

distance away from the centriole surface.

At times in the very early process of central spindle formation, we have observed the emanation of microtubule bundles from locations on the elongate-centriole at points somewhat proximal to the tip (Fig. 3*a, b*). This pattern is also reported by Cleveland (e.g. Fig. 76 in reference 4) and clearly illustrates an extensive microtubule organizing capability of the elongate-centriole. In addition to this activity at the distal, posterior end, the anterior end of the organelle organizes both the daughter elongate-centriole and the parabasal-axostylar lamella (4, 17, 25). For these reasons, we adhere to usage of the term elongate-centriole as originally designated by Cleveland even though the electron microscope has not revealed a "cartwheel" organization typical in centrioles of many cell types.³ It should be noted that one of us

³ We have not adopted Hollande and Valentin's term "pseudocentriole" (21) nor their term "attractophore" (fr. Gr. atraktos = spindle, arrow) proposed more recently (22, 23, 25). "Mimocentriole" (*mimo* = to mimic; kindly suggested by Drs. William Coleman and Camille Limoges of the History of Science Program, Marine Biological Laboratory, Woods Hole, Mass.) appeared better-suited until reviewing Boveri's definition of centriole. Apart from having priority, centriole is a workable term that will avoid needless confusion and plethora terminology otherwise designed to handle structural variations. Application of the term in this classical sense appears extensively in the literature of Boveri (2), who defined centriole, and of E. B. Wilson (44), Schrader (42), Cleveland, and countless others. Furthermore, Cleveland (4, 17) provided the first clear evidence for the dual functional nature of the centriole based in part on studies of *Barbulanympha*. However, in order not to imply the tubular cartwheel arrangement seen by electron microscopy in conventional centrioles, we have hyphenated elongate-centriole to make it a single term.

FIGURE 7 Mature central spindle in late prophase. Same spindle continued from Fig. 4, approximately one-half hour to 50 min later. (a), (b), (c), In polarized light with spindle axis oriented parallel to the polarizer. (d), (e), (f), Differential interference contrast displaying overlapping prophase chromosomes (*Ch*) whose dotlike kinetochores (*K*, see Part II Figs. 1, 9, 10) point to the spindle poles. Note also granules (*K?*) resembling kinetochores which stud the elongate-centrioles in (d) and (e). In (a), the distal portion of the left elongate-centriole (*E*) is in dark compensation, in (b) and (c) in bright compensation. The basal portion of the same elongate-centriole, which makes a right angle turn to the upper right and runs parallel to the parabasal axostylar lamella, is less clearly displayed but can be seen in reverse contrast (also, see Fig. 2 in Part II). The twisted course taken by the spindle fibers appears prominently in the polarized light images. See legend to Fig. 4 regarding the astral rays and chromosomal spindle fibers. *L*, polarizer and analyzer axes and quadrant containing slow axis of compensator. Time in h:min of day on 74g26. Bar, 30 $\mu\text{m} \times 690$.

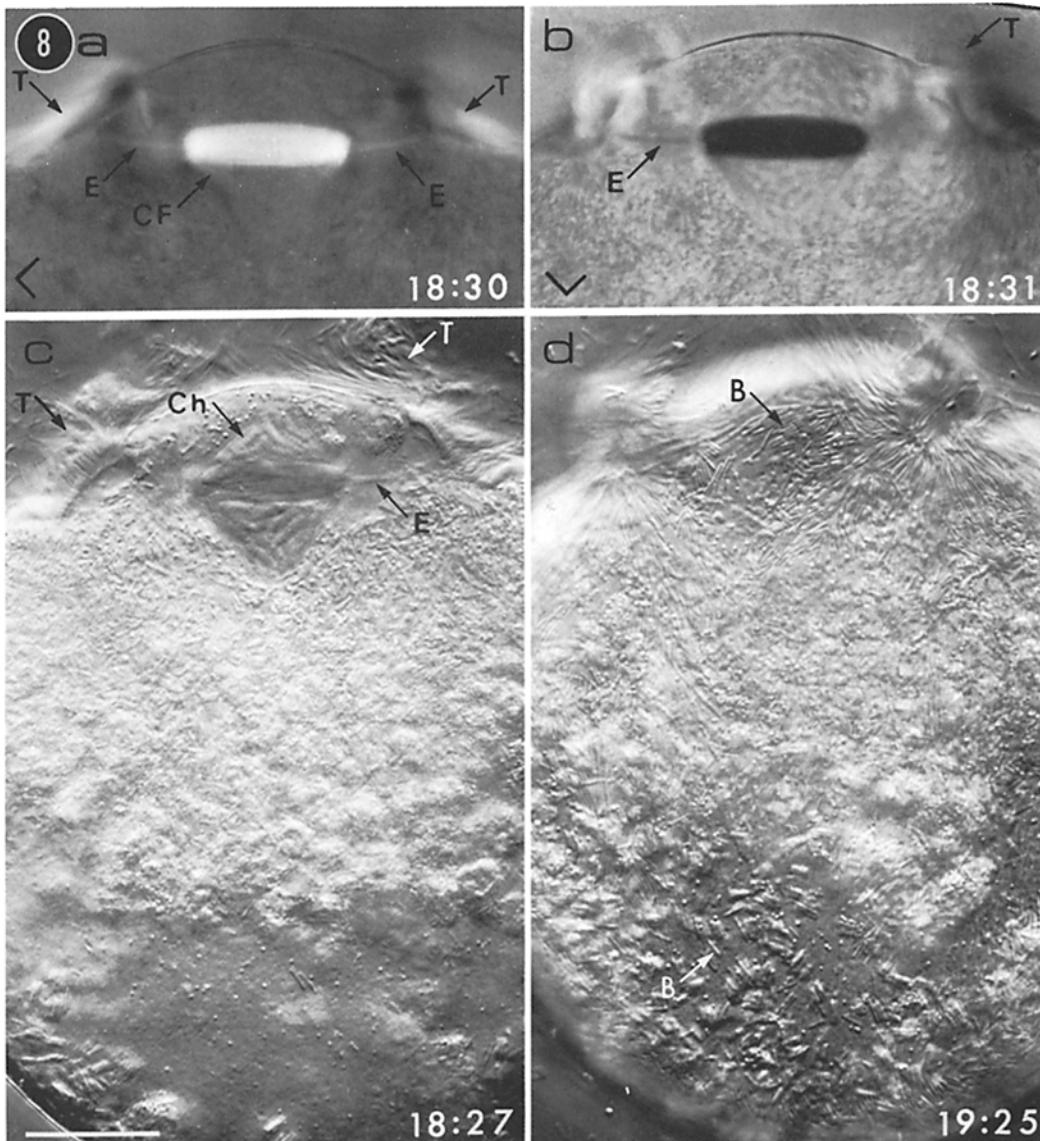


FIGURE 8 Mature central spindle of *Barbulanympha* in anaphase-A. (a), (b), In polarized light, with compensator orientation reversed. Flagellar tufts (*T*) are quite separated and the distal portions of the elongate-centrioles (*E*) now lie almost in line with the spindle. Short chromosomal spindle fibers (*CF*) run medially just below the spindle. (c), (d), Differential interference contrast view of the same cell. (c), Focused on right hand spindle pole and elongate-centriole. The nucleus has completely enveloped the central spindle so that chromosomes (*Ch*) are now seen anterior to the spindle as well as posteriorly. Chromosomes are in mid-anaphase-A; their tails have not yet separated. (d), Focused high on the same cell, showing characteristic, profuse bacterial growth (*B*) on the cell surface. h:min in time of day on 75h8. Continued to Figs. 4, 5, 6, and 7a in Part II. Bars, 30 μm . $\times 590$.

(D.K.) believes the microtubule organizing capability not to reside in the elongate-centriole proper but in a material closely ensheathing its fibrous core.

We have indicated that the movement of individual chromosomes and their kinetochores toward the poles is not always direct nor is it monotonic. These kinetochore movements, repet-

itively toward then away from the poles of the achromatic apparatus, suggest a shuttling process strongly resembling or even corresponding to the prometaphase activity seen in many other cell types. The fluctuation of birefringence seen as "Northern Lightslike" flickering in spermatocytes (28, 41), as well as shuttling activities of chromosomes (1, 18, 35) and perhaps also their prometaphase stretch (26), appear to reflect recurrent growth and contraction of the dynamic chromosomal spindle fibers.

In summary, we have succeeded in devising a long-awaited in vitro culture technique for *Cryptocercus* hindgut microorganisms, especially *Barbulanympha*. We have made use of through-focus serial recordings of living cells by rectified polarized light and differential interference contrast microscopy, supplemented by electron microscopy of thin sections. These advances have permitted us to describe the growth and establishment of the astral rays, central spindle fibers, and chromosomal fibers; the role played by the distal end of the elongate-centriole as an organizing center; the microscopic and fine structure of the anaphase-A central spindle; the engagement and forward hoisting of the nucleus via the kinetochores embedded in the nuclear envelope; and the dynamic features of recurrent transport of chromosomes via the kinetochores toward the spindle poles.

For our collection of *Cryptocercus*, we thank Susan Rogers and Catherine Sale who provided access to their Tumbling Waters property, Clayton, Georgia; also, the United States Department of the Interior, National Park Service for collecting permits specific for the Great Smoky Mountains National Park and the Asheville, Northern Carolina areas of the Blue Ridge Parkway.

The work reported in these two articles was supported in part by grants BMS 7500473 from the National Science Foundation and 5 R01 GM23475 from the National Institutes of Health awarded to Shiny Inoué. This work was also supported by the Office of General Research, University of Georgia, Athens, Georgia.

We thank the Rockefeller University Press for cooperating with us on experiments to optimize half-tone reproduction of polarization micrographs which contain extreme tonal ranges combined with subtle textural details. Based on these experiments, the micrographs in these two articles were skillfully printed by Christopher W. Inoué to optimize image sharpness and tonal ranges. Additionally, in Figs. 3c, 4a, b, 7a, b, and in Part II, Figs. 2a, e, f, 9e, 14a, c, e, and 15b and d, the very bright central spindle region was "burned in" to bring out image detail without other distortion of the image. Our thanks are also due Dr. Greenfield Sluder for help

on making the time-lapse motion picture which displayed chromosome churning in *Barbulanympha* anaphase. We are grateful to the staff of the Biophysical Cytology Program without whose dependent cooperation these reports would not have materialized.

Received for publication 29 July 1977, and in revised form 3 January 1978.

REFERENCES

1. BAJER, A. S., and J. MOLÈ-BAJER. 1972. Spindle dynamics and chromosome movements. *Int. Rev. Cytol.* **3** (Suppl.):1-271.
2. BOVERI, T. 1900. Über die Natur der Centrosomen. *Zellen-Studien*. Heft 4. Gustav Fischer Verlag KG. Jena, East Germany. 1-220.
3. BRINKLEY, B. R., and E. STUBBLEFIELD. 1970. Ultrastructure and interaction of the kinetochore and centriole in mitosis and meiosis. In *Advances in Cell Biology*, Vol. 1. D. M. Prescott, L. Goldstein, and E. McConkey, editors. Appleton-Century-Crofts, New York. 119-185.
4. CLEVELAND, L. R., S. R. HALL, E. P. SANDERS, and J. COLLIER. 1934. The wood-feeding roach *Cryptocercus*, its protozoa, and the symbiosis between protozoa and roach. *Mem. Am. Acad. Arts Sci.* **17**:185-342 (and 60 plates).
5. CLEVELAND, L. R. 1938. Origin and development of the achromatic figure. *Biol. Bull. (Woods Hole)*. **50**:41-55.
6. CLEVELAND, L. R. 1953. Hormone-induced sexual cycles of flagellates. IX. Haploid gametogenesis and fertilization in *Barbulanympha*. *J. Morphol.* **93**:371-404.
7. CLEVELAND, L. R. 1953. Studies on chromosomes and nuclear division. IV. Photomicrographs of living cells during meiotic divisions. *Trans. Am. Philos. Soc.* **43**:848-869.
8. CLEVELAND, L. R. 1954. Hormone-induced sexual cycles of flagellates. X. Autogamy and endomitosis in *Barbulanympha* resulting from interruption of haploid gametogenesis. *J. Morphol.* **95**:189-212.
9. CLEVELAND, L. R. 1954. Hormone-induced sexual cycles of flagellates. XI. Reorganization in the zygote of *Barbulanympha* without nuclear or cytoplasmic division. *J. Morphol.* **95**:213-235.
10. CLEVELAND, L. R. 1954. Hormone-induced sexual cycles of flagellates. XII. Meiosis in *Barbulanympha* following fertilization, autogamy and endomitosis. *J. Morphol.* **95**:557-620.
11. CLEVELAND, L. R. 1955. Hormone-induced sexual cycles of flagellates. XIII. Unusual behavior of gametes and centrioles of *Barbulanympha*. *J. Morphol.* **97**:511-542.
12. CLEVELAND, L. R. 1956. Effects of temperature and tension on oxygen toxicity for the protozoa of *Cryptocercus*. *J. Protozool.* **3**:74-77.

13. CLEVELAND, L. R. 1957. Correlation between the molting period of *Cryptocercus* and sexuality in its protozoa. *J. Protozool.* **4**:168-175.
14. CLEVELAND, L. R. 1957. Achromatic figure formation by multiple centrioles of *Barbulanympha*. *J. Protozool.* **4**:241-248.
15. CLEVELAND, L. R. 1958. A factual analysis of chromosomal movement in *Barbulanympha*. *J. Protozool.* **5**:47-62.
16. CLEVELAND, L. R. 1959. Sex induced with ecdysone. *Proc. Natl. Acad. Sci. U. S. A.* **45**:747-753.
17. CLEVELAND, L. R. 1963. Functions of flagellate and other centrioles in cell reproduction. In *The Cell in Mitosis*. L. Levine, editor. Academic Press, Inc., New York. 3-31.
18. DIETZ, R. 1969. Bau and Funktion des Spindelapparats. *Naturwissenschaften.* **56**:237-248.
19. DVORAK, J. A., and W. F. STOTLER. 1971. A controlled-environment culture system for high resolution light microscopy. *Exp. Cell Res.* **68**:144-148.
20. FUSELER, J. W. 1975. Mitosis in *Tilia americana* endosperm. *J. Cell Biol.* **64**:159-171.
21. HOLLANDE, A., and J. VALENTIN. 1967. Interprétation des structures dites centriolaires chez les Hypermastigines symbiontes des Termites et du *Cryptocercus*. *C. R. Acad. Sci.* **264**:1868-1871.
22. HOLLANDE, A., and J. VALENTIN. 1967. Relations entre cinéosomes, "attractophores" et complexe fibrillaire axostyloparabasal, chez les Hypermastigines du genre *Barbulanympha*. *C.R. Acad. Sci.* **264**:3020-3022.
23. HOLLANDE, A., and J. VALENTIN. 1967. Morphologie et infrastructure du genre *Barbulanympha*, hypermastigine symbiontique de *Cryptocercus punctulatus* Scudder. *Protistologica.* **3**:257-267 (and 11 plates).
24. HOLLANDE, A., and J. VALENTIN. 1968. Infrastructure des centromères et déroulement de la pleuromitose chez les Hypermastigines. *C.R. Acad. Sci.* **266**:367-370.
25. HOLLANDE, A., and J. CARRUETTE-VALENTIN. 1971. Les attractophores, l'induction du fuseau et la division cellulaire chez les Hypermastigines. Étude infrastructurale et révision systématique des Trichonymphines et des Spirotrichonymphines. *Protistologica.* **7**:5-100.
26. HUGHES-SCHRADER, S. 1947. The "pre-metaphase stretch" and kinetochore orientation in phasmids. *Chromosoma (Berl.)*. **3**:1-21.
27. HUGHES, A. F., and M. M. SWANN. 1948. Anaphase movements in the living cell. A study with phase contrast and polarized light on chick tissue cultures. *J. Exp. Biol.*, **25**:45-70 (and 2 plates.).
28. INOUÉ, S. 1964. Organization and function of the mitotic spindle. In *Primitive Motile Systems in Cell Biology*. R. D. Allen and N. Kamiya, editors. Academic Press, Inc., New York 549-598.
29. INOUÉ, S. 1969. The physics of structural organization in living cells. In *Biology and the Physical Sciences*. Samuel Devons, editor. Columbia University Press, New York. 139-171.
30. INOUÉ, S. 1961. Polarizing microscope: design for maximum sensitivity. In *The Encyclopedia of Microscopy*. G. L. Clarke, editor. Reinhold Publishing Corp., New York. 480-485.
31. INOUÉ, S., and W. L. HYDE. 1957. Studies on depolarization of light at microscope lens surfaces. II. The simultaneous realization of high resolution and high sensitivity with the polarizing microscope. *J. Biophys. Biochem. Cytol.* **3**:831-838.
32. INOUÉ, S., and H. RITTER, JR. 1975. Dynamics of mitotic spindle organization and function. In *Molecules and Cell Movement*. S. Inoué and R. E. Stephens, editors. Raven Press, New York. 3-30.
33. KUBAI, D. F. 1973. Unorthodox mitosis in *Trichonympha agilis*: kinetochore differentiation and chromosome movement. *J. Cell Sci.* **13**:511-552.
34. MCKITTRICK, F. A. 1964. Evolutionary studies of cockroaches. Memoir 389. Cornell Univ. Agr. Exp. Sta. Ithaca, N. Y. 1-197.
35. NICKLAS, R. B. 1971. Mitosis. In *Advances in Cell Biology*, Vol. 2. D. M. Prescott, L. Goldstein, and E. McConkey, editors. Appleton-Century-Crofts, New York. 225-297.
36. RITTER, H. 1961. Glutathione-controlled anaerobiosis in *Cryptocercus* and its detection by polarography. *Biol. Bull. (Woods Hole)*. **121**:330-346.
37. RITTER, H. 1974. A fluid system for the cultivation, light microscope examination and manipulation of obligate anaerobes. *J. Protozool.* **21**:565-568.
38. RITTER, H., and W. J. HUMPHREYS. 1971. A cell membrane adhering bacterial symbiont of the flagellate protozoan *Barbulanympha*, a mutualist in the hind-gut of the wood-feeding cockroach *Cryptocercus*. Proceedings of the 11th Annual Meeting of the American Society for Cell Biology. **51**:247a. (Abstr.).
39. SATO, H. 1975. The mitotic spindle. In *Aging Gametes*. R. J. Blandau, editor. Karger AG., S. Basel, Switzerland. 19-49.
40. SATO, H., G. W. ELLIS, and S. INOUÉ. 1975. Microtubular origin of mitotic spindle form birefringence. *J. Cell Biol.* **67**:501-517.
41. SATO, H., and K. IZUTSU. 1974. Birefringence in Meiosis of Grasshopper Spermatocytes: *Chrysochraon japonicus* and *Trilophidia annulata*. Time-lapse motion picture. Available from George W. Colburn Laboratory, Inc., Chicago, Illinois 60606.
42. SCHRADER, F. 1953. Mitosis: The Movements of Chromosomes in Cell Division. Columbia University Press, New York 2nd edition. 1-170.
43. WENT, H. A. 1966. The behavior of centrioles and the structure and formation of the achromatic figure. *Protoplasmatologia.* **6**:1-109.
44. WILSON, E. B. 1925. The Cell in Development and Heredity. Macmillan, Inc., New York 3rd edition. 1-1232.